Volume 153
Number 1
April 2, 2001
Published by
The Rockefeller
University Press
http://www.jcb.org

The Journal of Cell Biology

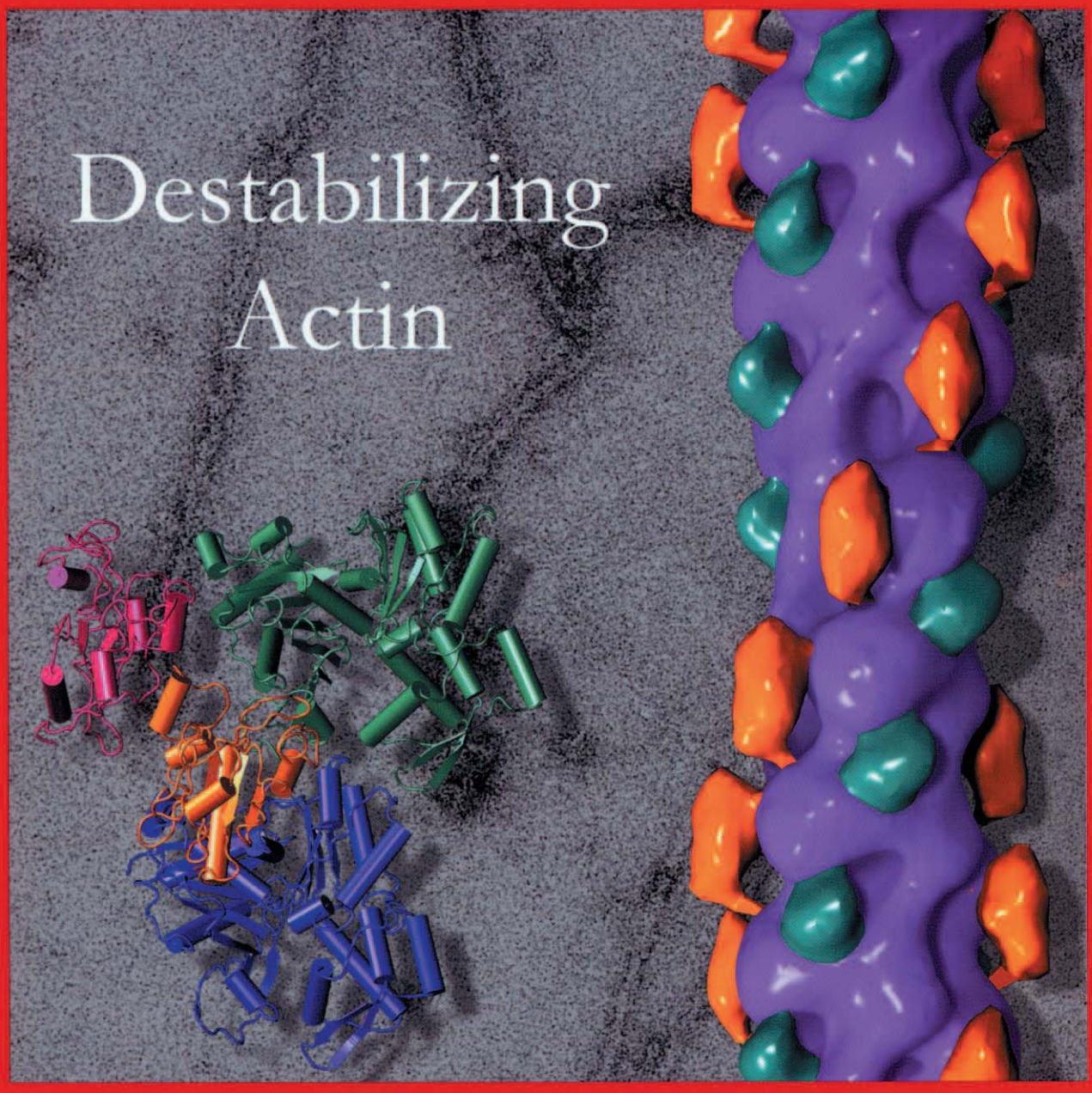

Actin Depolymerizing Factor Stabilizes an Existing State of F-Actin and Can Change the Tilt of F-Actin Subunits

Vitold E. Galkin,*‡ Albina Orlova,* Natalya Lukoyanova,*§ Willy Wriggers,‖ and Edward H. Egelman*

*Department of Biochemistry and Molecular Genetics, University of Virginia Health Sciences Center, Charlottesville, Virginia 22908; ‡Department of Cell Cultures, Institute of Cytology RAS, St. Petersburg, Russia; §Institute of Theoretical and Experimental Biophysics RAS, Puschino, Russia; ‖Department of Molecular Biology, The Scripps Research Institute, La Jolla, California 92037

Abstract. Proteins in the actin depolymerizing factor (ADF)/cofilin family are essential for rapid F-actin turnover, and most depolymerize actin in a pH-dependent manner. Complexes of human and plant ADF with F-actin at different pH were examined using electron microscopy and a novel method of image analysis for helical filaments. Although ADF changes the mean twist of actin, we show that it does this by stabilizing a preexisting F-actin angular conformation. In addition, ADF induces a large (~12°) tilt of actin subunits at high pH where filaments are readily disrupted. A second ADF molecule binds to a site on the opposite side of F-actin from that of the previously described ADF binding site, and this second site is only largely occupied at high pH. All of these states display a high degree of cooperativity that appears to be an integral part of F-actin.

Key words: actin • ADF • cooperativity • electron microscopy • image processing

Introduction

Actin dynamics play a major role in cell motility, cytokinesis, and endocytosis. The rapid polymerization/depolymerization of actin filaments in the cell, especially under the leading membrane edge, requires an efficient protein machinery that can provide a fast response to extracellular stimuli (Chen et al., 2000; Pollard et al., 2000). A large number of actin binding proteins have been shown to participate in the assembly, disassembly, and rearrangement of the cytoskeleton. Proteins in the actin depolymerizing factor (ADF)[1]/cofilin family are essential, conserved, and widespread actin depolymerizing factors that interact with F-actin in a strong cooperative manner (Hawkins et al., 1993; Hayden et al., 1993; Blanchoin and Pollard, 1999). All members of the ADF/cofilin family are small proteins that contain between 118 and 168 amino acids (13–19 kD), and most depolymerize actin more rapidly at higher pH (Yonezawa et al., 1985; Bernstein et al., 2000). The exceptions to this pH dependence are *Acanthamoeba* actophorin (Maciver et al., 1998) and starfish depactin (Bamburg et al., 1999). ADF and cofilin from a single organism share ~70% sequence identity, whereas the difference between ADFs from different organisms is much higher (Bamburg, 1999). In this work, we used plant *Acanthamoeba thaliana* ADF1 (p-ADF) and human ADF (h-ADF), molecules that share only 31% identity.

Two possible mechanisms of actin depolymerization were proposed for ADF/cofilin proteins. It was suggested that ADF depolymerizes actin due to a severing activity (Cooper et al., 1986; Maciver et al., 1991). Carlier (1998) proposed that the acceleration of treadmilling via the enhancement of the off-rate at the barbed end of the filament by ADF/cofilin proteins is responsible for actin filament destabilization (Carlier and Pantaloni, 1997). A combination of both mechanisms has also been suggested (Theriot, 1997), and the main question involves the relative contribution of each of these mechanisms to actin filament shortening (Du and Frieden, 1998; Moriyama and Yahara, 1999).

A growing body of evidence suggests that the geometry and internal dynamics of actin filaments might be functionally important in the interaction between F-actin and many actin-binding proteins. For example, in muscle, it has been shown using mutations (Drummond et al., 1990), cross-linking (Prochniewicz and Yanagida, 1990; Kim et al., 1998), and proteolysis (Schwyter et al., 1990) that modifications can be made to F-actin that do not prevent the binding of myosin and do not inhibit the activation of myosin's ATPase activity but do prevent the generation of force. The variability in the structure of F-actin may be important in this context. In an ideal actin filament, actin subunits are related to each other by an axial rise of 27 Å

Address correspondence to Edward H. Egelman, Department of Biochemistry and Molecular Genetics, Box 800733, University of Virginia Health Sciences Center, Charlottesville, VA 22908-0733. Tel.: (804) 924-8210. Fax: (804) 924-5069. E-mail: egelman@virginia.edu

[1]*Abbreviations used in this paper:* ADF, actin depolymerizing factor; h-ADF, human ADF; IHRSR, iterative helical real space reconstruction; p-ADF, plant *A. thaliana* ADF1.

and a rotation of ~167°. This symmetry operation can generate every subunit in a filament, given a single subunit. Because subunit *n* will be rotated ~26° from both subunits $n - 2$ and $n + 2$, the resulting filament can also be described by a helix containing two ~700-Å-pitch axially staggered strands that crossover in projection at average intervals of ~350 Å. However, early electron microscopic observations showed that the actual crossover points of negatively stained actin filaments were far from uniform in their length (Hanson, 1967). A subsequent model suggested that this arises from an unusual property of F-actin where subunits have the ability to rotate within the filaments, although the axial rise per subunit is quite fixed (Egelman et al., 1982). It was proposed that this rotational variability of F-actin might help the cell to use a single highly conserved protein in several different structures. Human cofilin was observed to change the twist of actin by ~5° per subunit when it was bound stoichiometrically to F-actin (McGough et al., 1997), and it was proposed that this change in actin symmetry was responsible for the destabilization of the actin filament. Later, using a mutant cofilin that bound to actin but did not destabilize the filament, it was suggested that the change in twist induced by cofilin could be uncoupled from subunit dissociation (Pope et al., 2000). Thus, there is no clear picture for the role of the change in actin's twist in the mechanism of ADF/cofilin-induced actin depolymerization.

We have used a new approach for image analysis of helical filaments (Egelman, 2000) to examine both pure actin filaments and complexes of F-actin with p- and h-ADF. This new approach allows us to analyze tens of thousands of short segments within filaments, without the need to assume a fixed helical symmetry for a long filament. This approach is therefore sensitive to variations in helical symmetry between different segments, as well as to differences in the occupancy of the ADF molecules bound to F-actin. Using this method, we show that segments of pure actin can be found in an ADF/cofilin-like state of twist in the absence of other proteins. Furthermore, the ADF–actin complex can exist with a twist close to that of the normal actin state. We find that under conditions where actin filaments are readily depolymerized, two molecules of ADF bind per actin subunit, and not one as has been believed previously. We also find that under these conditions of filament destabilization some actin subunits undergo a large tilt from their positions in normal F-actin that causes the breakage of the longitudinal contacts within the actin filament. These results provide new insight into the internal dynamics of F-actin, suggesting that they may be even larger in magnitude than previously imagined, and suggest that certain actin-binding proteins in the cell may have evolved to regulate these internal dynamics as part of cellular control of the cytoskeleton.

Materials and Methods

Protein Preparation and EM

Actin was prepared from rabbit skeletal muscle (Strzelecka-Golaszewska et al., 1980) and isolated as Ca^{2+}–G-actin by chromatography over a Superdex-200 column using the AKTA Explorer HPLC system (Amersham Pharmacia Biotech). G–Ca^{2+}–actin was diluted to a final concentration of 0.5 mg/ml by 5 mM Pipes buffer, pH 6.5, or 5 mM Tris buffer, pH 7.7. Ca^{2+} was replaced with Mg^{2+} by incubating G-actin with 0.2 mM EGTA and 0.2 mM $MgCl_2$ for 10 min at room temperature. G-actins were polymerized by 0.1 M KCl and 2 mM $MgCl_2$ by incubating 2 h at room temperature and then overnight at 4°C. F-actins were spun down in a TLX-120 tabletop ultracentrifuge (Beckman Coulter), and pellets were homogenized in fresh F buffers (0.1 mM KCl, 1 mM $MgCl_2$, 15 mM Tris buffer, pH 7.7, or Pipes buffer, pH 6.5) and diluted to final concentrations of 2–4 μM. p-ADF (Carlier et al., 1997) and h-ADF were a gift from Dr. M.-F. Carlier (Laboratory of Enzymology and Structural Biochemistry, Gif-Sur-Yvette, France). ADFs were diluted by F buffers to final concentrations of 3–6 μM.

Negatively stained samples were prepared by incubation for 10 min in tubes of 2 μM actin with 6 μM ADF or by decoration on the grid, where one drop (6 μl) of 2 μM actin was applied to 300-mesh copper grids coated with carbon for 1 min, and then two separate drops (6 μl each) of 4 μM ADF were added for 30 s–2 min. The grids were rinsed with two drops of 1% uranyl acetate.

Specimens were examined in a JEOL 1200 EX11 electron microscope at an accelerating voltage of 80 kV and a nominal magnification of 30,000×. Negatives were densitometered with a Leaf 45 scanner, using a raster of 4 Å/pixel.

Image Analysis

The references for initial multireference cross-correlation analysis were generated using layer lines extracted from an atomic model of the F-actin filament (Holmes et al., 1990). The symmetry of this model was changed by reindexing the layer lines (from a 13/6 helix): $l = 0$, $n = 0$; $l = 1$, $n = 2$; $l = 2$, $n = 4$; $l = 3$, $n = 6$; $l = 4$, $n = -5$; $l = 5$, $n = -3$; $l = 6$, $n = -1$; $l = 7$, $n = 1$; $l = 8$, $n = 3$; $l = 12$, $n = -2$; $l = 13$, $n = 0$; $l = 14$, $n = 2$. The subsequent procedure for iterative helical real space reconstruction was as described (Egelman, 2000). Segments of pure F-actin and F-ADF–actin complexes were placed in 100 × 100 pixel boxes (~400 × 400 Å), and these were cross-correlated against reference projections using a real space radius of 42 pixels in the search. Thus, the cross-correlation search involved ~12 subunits. The search for helical symmetry within the asymmetric volume generated by back-projection involved nine subunits, eliminating possible end effects that are present due to the geometry of the reconstruction (Egelman, 2000). Typically, ~10% of filament segments were excluded during the iterations, based on poor cross-correlations against the reference volumes. The resolution of the reconstructions was determined by generating two independent reconstructions from each data set after randomly dividing the images into two equal subsets. The correlation coefficients from each of these pairs of reconstructions was >0.5 with a resolution of ≤25 Å for the ADF–actin complexes and ≤30 Å for both the pure and naked actin. Using the 3σ criterion (Saxton and Baumeister, 1982) rather than the correlation coefficient, the estimate for resolution is ~20 Å for the ADF–actin complexes and ~25 Å for both the pure and naked actin.

The cross-correlation procedure was used to discriminate ADF-bound and naked actin segments in a similar manner to that described for sorting by symmetry. We term actin "naked" when patches of undecorated actin are found within ADF-decorated actin filaments, in contrast to "pure" F-actin, which refers to actin filaments in the absence of any additional proteins. References were created by imposing a symmetry of 162.0° on the pure F-actin reconstruction as well as on the fully ADF-decorated F-actin to distinguish segments by the presence or absence of the ADF, rather than by symmetry. The reconstruction algorithm was then iterated many times in each cycle, eliminating those segments that had a poor cross-correlation coefficient against the continuously updated naked actin reconstruction. This was continued (for 60–250 cycles) until a stable solution was found with respect to both symmetry and the number of segments identified as naked actin. The validation of this sorting procedure was that reconstructions of segments from ADF-decorated filaments that were selected by higher cross-correlation against the pure F-actin reference than against the ADF–actin reference looked like undecorated actin.

Surface thresholds were determined by using 125% of the expected molecular volume of pure actin, and 100% of the expected molecular volume for both the 1:1 or 2:1 ADF–actin complexes, assuming a partial specific volume of protein of 0.75 cm^3/g.

Fitting of Actin and ADF Monomer Structures

The missing DNase-1 binding loop was added to the actin structure (Protein Data Bank entry 1EQY) as described (Wriggers and Schulten, 1999). h-ADF coordinates were obtained from PDB entry 1AK6 (Hatanaka et al., 1996). The fitting of atomic models into EM reconstructions was car-

ried out with the Situs package v1.4 (Wriggers et al., 1999). The fitting method takes advantage of topology-representing neural networks that represent the shape features and three-dimensional density distribution of both atomic and low-resolution data by a discrete number of vectors (Wriggers et al., 1998). It was shown that this docking approach reconstructs atomic models of undecorated actin filament structures with a precision of one order of magnitude above the nominal resolution of the underlying low-resolution map (Wriggers et al., 1999). The main innovation implemented in Situs v1.4 is the addition of distance constraints between adjacent vectors. The resulting distance-constrained vectors freeze the degrees of freedom that are inessential for the docking and thereby provide robustness against the effects of noise and experimental uncertainty (Wriggers and Birmanns, 2001). Five vectors were used per actin subunit, and two vectors per ADF molecule. Helical boundary conditions were applied. Since rigid body docking was performed, intramolecular distances (derived from the atomic structures) were constrained, using the SHAKE algorithm (van Gunsteren and Berendsen, 1977), whereas intermolecular distances remained free. The resulting vectors provided anchor points for a least squares fitting of individual molecules (Wriggers et al., 1998).

To test the fitting algorithm for the ADF-decorated volume, we compared the model resulting from a fit of G-actin to the ADF-decorated volume with the Holmes model. The root mean square deviation of the resulting model from the symmetry corrected Holmes model was only 1.76 Å, demonstrating the reliability of the skeleton-based docking approach. After the docking of actin, the resolution of the resulting F-actin model was lowered to 20 Å using the Situs pdblur utility (Wriggers and Birmanns, 2001). The amplitude of the simulated actin map was varied systematically to match the actin surface in the experimental map at like threshold levels. Subsequently, the simulated actin map was subtracted from the experimental data set. Single molecule densities of the primary and secondary ADF molecules were isolated with Situs as described (Wriggers et al., 1999). Finally, the ADF structure was docked to the single molecule densities. There was a sixfold degeneracy in the vector rms deviation score for the primary ADF, but only one of the possible solutions was consistent with the biochemical information on the consensus binding interface with actin (Yonezawa et al., 1991; Lappalainen et al., 1997; Van Troys et al., 1997; Ono et al., 1999). The shape-based docking was unambiguous in the case of the second ADF, and no biochemical data was used in this case to help orient the molecule.

Results

Rotational Variability of Pure F-Actin Allows It to Exist in the ADF/Cofilin-like Twist State

The unusual twist previously reported for cofilin-decorated actin filaments (changing F-actin from ~167°–162° of rotation per subunit) was observed at pH 6.6 where stable filaments of actin–cofilin complex can be observed (McGough et al., 1997). At higher pH, cofilin will depolymerize actin filaments more efficiently. To determine the distribution of filament twist for pure F-actin at low pH, we examined 10,800 segments of Mg^{2+}–F-actin polymerized at pH 6.5. The frequency distribution of the images according to their twist (Fig. 1 a) is based on finding which of 27 reference filaments with angular rotations per subunit of 152°–179° generates the highest cross-correlation when projections of the references are compared with the raw images. This distribution is extremely broad, and the dispersion has two components: the intrinsic variability of the twist of pure F-actin (Egelman et al., 1982), and the poor signal-to-noise ratio present in segments of F-actin that contain only ~12 subunits. Model calculations show, as expected, that the dispersion in cross-correlation against references with different symmetries will increase as the signal-to-noise ratio is decreased. The iterative helical real space reconstruction (IHRSR) method (Egelman, 2000), however, allows us to take subsets sorted as shown in Fig. 1 a and find if they yield a stable solution. The subsets from the far left (<156°) and the far right (>170°) of the distribution gave symmetries, after multiple iterations, that were either close to the central part of the distribution or had no stable solution. Thus, we can dismiss those outlying symmetries as being due to errors in the initial sorting by twist because of noise or heterogeneity.

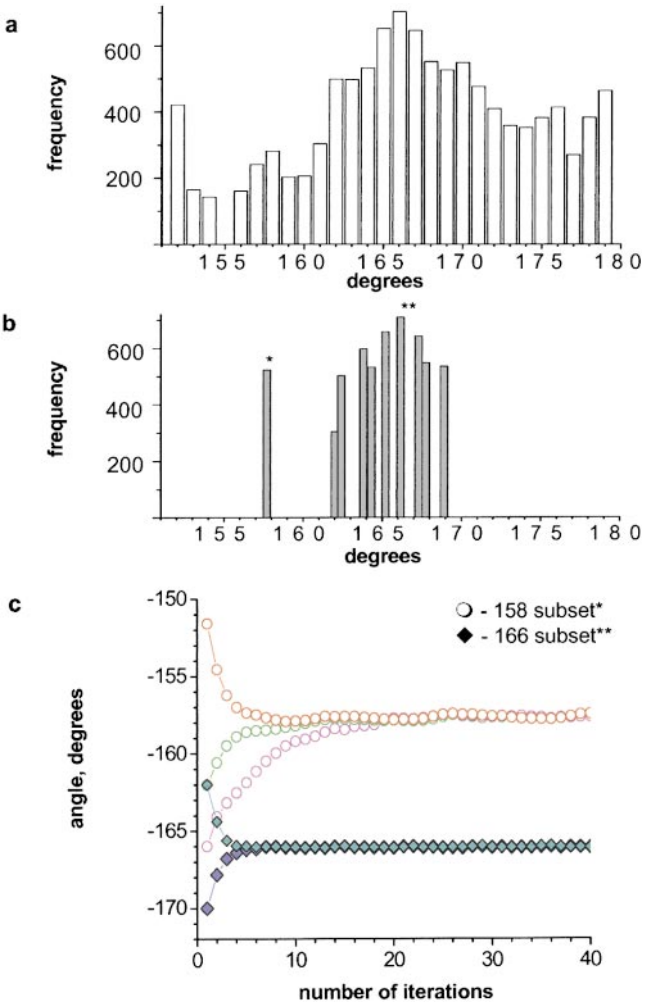

Figure 1. Variability in twist of pure Mg^{2+}-actin at pH 6.5. (a) The distribution of mean twist angles in 10,800 segments of Mg^{2+}-actin at pH 6.5 observed by multireference cross-correlation analysis. The 27 different references were generated by using 152°–179° of rotation per subunit in a low-resolution version of an atomic model of the actin filament (Holmes et al., 1990). Each reference volume was rotated by 4° increments about the filament axis and projected onto a plane, to generate 90 images. These 2,430 (27 × 90) reference projections were used to sort the raw images by symmetry. (b) Final distribution of angles in Mg^{2+}-actin at pH 6.5, based on stable solutions for subsets from distribution (a) found by the IHRSR method (Egelman, 2000). (c) The operational definition of a stable solution is that subsets converge to the same solution for helical symmetry from different starting points. This is shown for the 158° and 166° subsets.

The frequency distribution of stable solutions (Fig. 1 b) must be an underestimate of the dispersion of average twist of filament segments containing ~12 subunits. The reason that this is an underestimate is due to the way that these solutions have been obtained. We consider a solution stable if we can show that it converges to a particular

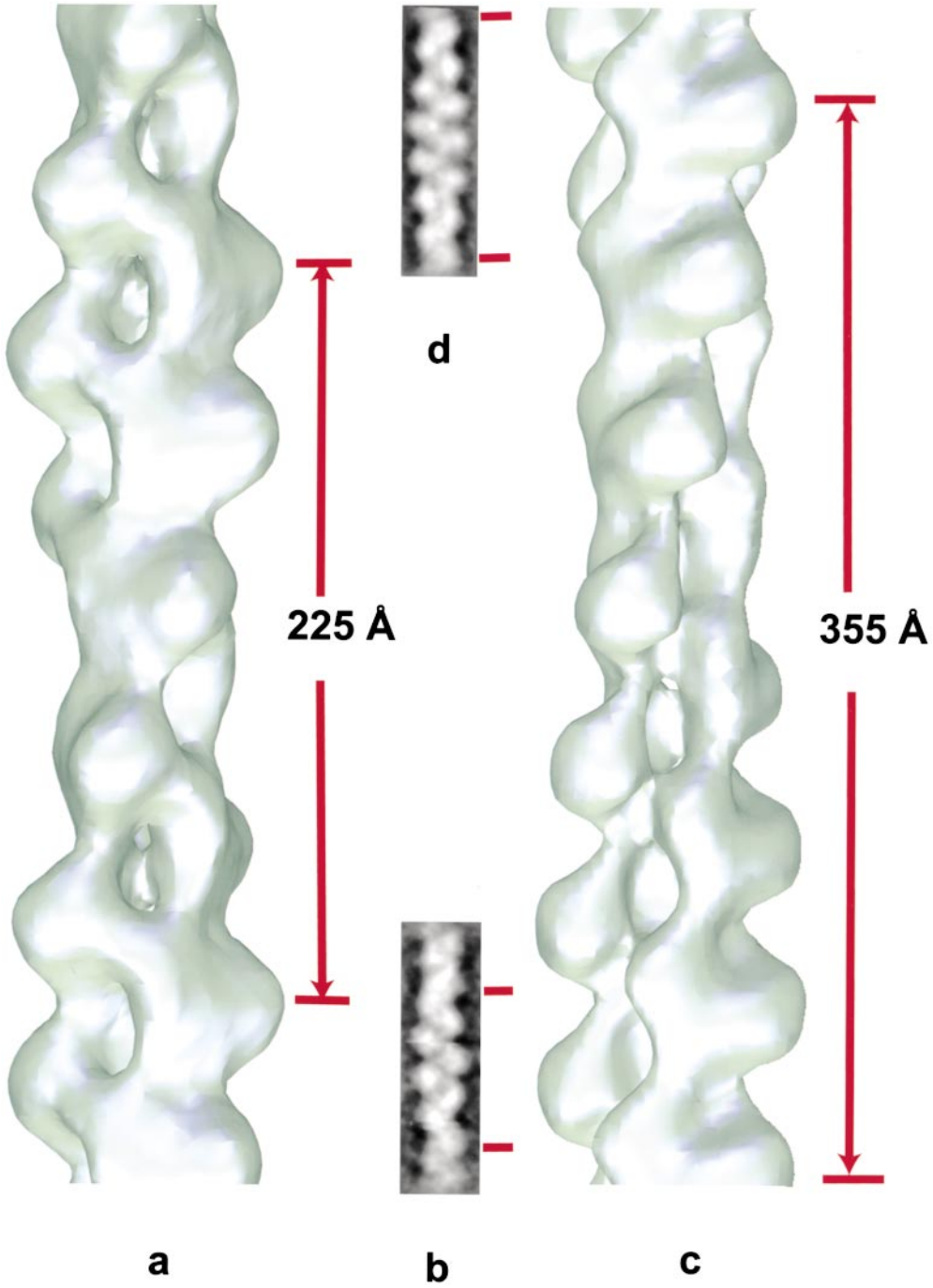

Figure 2. Reconstruction of two twist states of pure F-actin at pH 6.5. Filament segments from the 158° subset (a; $n = 523$) and the 166° subset (c; $n = 709$) of Fig. 1 b have been reconstructed using IHRSR. The long-pitch actin helix in panel a undergoes a 180° rotation in 225 Å, whereas this helix undergoes the same rotation in 355 Å in (c). Two-dimensional averages from these subsets are shown in b and d, where the large differences in cross-over spacings (marked by bars) can be easily seen.

helical symmetry independent of the starting point for the iterative procedure. Fig. 1 c illustrates this for two different subsets, 158° and 166°. It can be seen, for example, that the 158° solution is reached whether the iterations are started from a model having 151.5°, 162°, or 166° rotation per subunit. Similarly, the 166° solution is found whether the iterations start from 162° or 170°. Thus, we have high confidence that each stable solution corresponds to a real state for the average twist of 12 F-actin subunits, but we cannot exclude the possibility that other average states, further from the mean, actually exist. When the entire data set was combined, an overall symmetry of 166.1° was found. Keeping in mind that cofilin changes the mean twist of actin filaments to ~162° (McGough et al., 1997), it can be seen (Fig. 1 b) that ~5–10% of segments of pure F-actin can be found with a mean twist of 162°, or even 158°, without ADF/cofilin bound. Since the 158° state is so far from anything that has been described previously, we were interested to see if this was associated with filament ends, because the untwisting of actin was proposed as a mechanism of actin depolymerization (McGough et al., 1997). By selecting segments that were only close to filament ends, we did not see any significant increase in the frequency of this state. Our results suggest that these segments are randomly distributed within actin filaments.

The three-dimensional reconstructions of pure actin from the 158° subset (Fig. 2 a) and from the 166° subset (Fig. 2 c) obtained by the IHRSR method have an obviously different twist. To exclude the possibility that this difference in twist is an artifact of the three-dimensional reconstruction

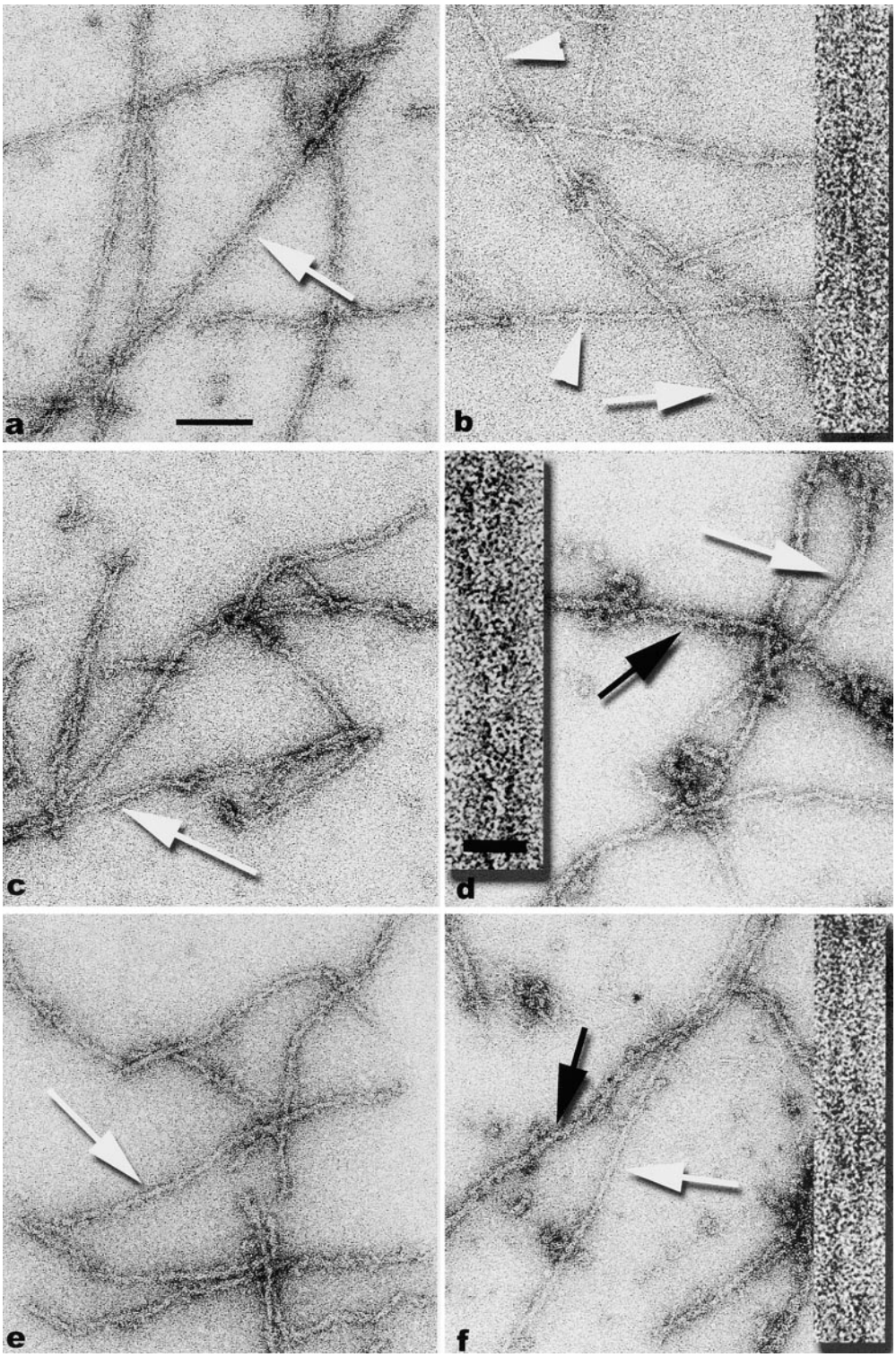

Figure 3. Electron micrographs of p- (a, c, and e) and h-ADF (b, d, and f) complexes with F-actin. F-actin was incubated for 2 min with p- (a) or h-ADF (b) on the EM grid at pH 6.5 for 2 min. F-actin was incubated in a tube for 10 min with p- (c) or h-ADF (d) at pH 6.5. F-actin was incubated on the EM grid with p-ADF (e) or h-ADF (f) at pH 7.7 for 2 min. White arrowheads (b) indicate undecorated actin filaments. The enlarged view of such a filament is shown as inset in b. Black arrows indicate darkly stained regions (d and f) and shown as an inset in d. ADF–actin filaments with light staining are marked with white arrows (c–f) and insert in f. Bars: (a) 1,000 Å; (d, inset) 300 Å.

method, actin images from each of the two sets were averaged together. The resulting two-dimensional averages (Fig. 2, b and d) have approximately the same difference in crossover lengths, as can be seen in the three-dimensional reconstructions (Fig. 2, a and c). We have also used cryo-EM on unstained frozen-hydrated actin filaments and find a similar distribution of twist (data not shown), excluding the possibility that the variation in twist is due to specimen preparation. Thus, cofilin/ADF do not induce a new state of twist in F-actin, but either stabilize a particular state of twist in which pure actin can be found or shift the overall distribution of twist by ~5°. The results below suggest that the former possibility is more likely.

Symmetry of ADF–Actin Complexes

h-ADF is more efficient at disrupting rabbit muscle actin filaments than is p-ADF, and this difference is more obvious at high pH (Ressad et al., 1998). We have therefore used incubations of p- and h-ADF with F-actin at both pH 6.5 and 7.7 (Fig. 3). We observed that h-ADF bound to F-actin at pH 6.5 more slowly than p-ADF (Fig. 3, com-

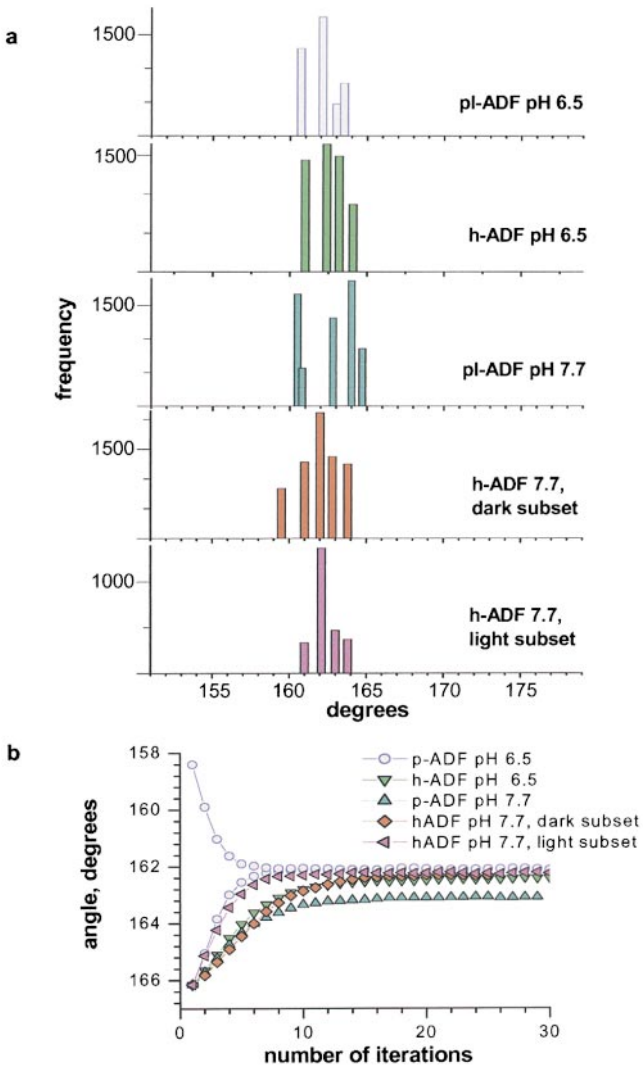

Figure 4. Rotational variability of ADF–actin complex at pH 6.5 and 7.7. (a) The distribution of angles in ADF–actin complexes at pH 6.5 and 7.7, observed by cross-correlation analysis and the formation of stable subsets as was described for Fig. 1. (b) All ADF–actin sets converge to a symmetry of ~162° in the IHRSR approach, except the p-ADF–actin complex at pH 7.7, which has a twist of ~163°. The stability of solutions in the IHRSR application to ADF–actin complexes is shown for the p-ADF–actin complex at pH 6.5, which converges from both 158° and 166° starting points to a twist of 162°.

pare a with b). After 2 min of incubation on the grid, filaments were fully decorated with p-ADF, but only partial decoration was noticed for h-ADF. Full occupancy was reached for h-ADF only after 10 min of incubation (Fig. 3 d). There were no differences in EM pictures between p-ADF–decorated actin after 2 min incubation on the grid or 10 min incubation in tubes, except filaments were shorter after the longer incubation (Fig. 3, a and c). But h-ADF–decorated F-actin appeared quite different from p-ADF after 2 min incubation on the grid, as well as after 10 min incubation in tubes (Fig. 3, compare a, c, and d). Approximately 30% of filaments decorated with h-ADF appeared more massive and were stained more darkly (Fig. 3 d, black arrow), and no such filaments were found in p-ADF samples. For h-ADF–actin filaments at pH 7.7, ~70% were darkly stained (Fig. 3 f, black arrow), as opposed to ~30% found at ph 6.5 (Fig. 3 d, black arrow). No filaments containing regions of both dark and light staining were found. The pH 7.7 h-ADF–actin filaments were sorted into two subsets, based upon this staining, before subsequent image analysis.

Stable solutions were sought for p-ADF and h-ADF complexes with F-actin at both pH 6.5 and 7.7, after the procedure described for pure F-actin, and these are shown in Fig. 4 a. Several contrasts exist with the distribution for pure F-actin (Fig. 1 b). The means of the twist distribution for all ADF–actin complexes were ~162°, but segments of actin filaments decorated with ADF could also be found in states with an average twist of 164°–165°, close to the normal F-actin twist. The dispersion in the twist distributions is greatly reduced compared with pure F-actin, consistent with the notion that ADF may be preferentially stabilizing an existing state or states of F-actin out of several possible states. By combining all images from each group, rather than searching for subsets that yielded stable solutions, the overall symmetries all converged to ~162°, except for the p-ADF complex, pH 7.7, where the average symmetry was ~163°.

Reconstruction of the ADF–F-Actin Complexes by the Single Particle Approach

Three-dimensional reconstructions were generated for different subsets of the ADF–actin complexes using the IHRSR method (Fig. 5). To assist in interpreting the mass due to ADF, we have superimposed an ADF–actin, pH 6.5, reconstruction (Fig. 5 c) on a pure F-actin reconstruction (Fig. 5 a), and the difference density in Fig. 5 b is very similar to what has previously been described for cofilin (McGough et al., 1997). The most striking difference with previous work, however, is the visualization of a second h-ADF molecule bound to a site on the opposite side of the actin subunit from the primary ADF. This second h-ADF can be seen partially in Fig. 5 d (pH 6.5) and more fully in Fig. 5 f (pH 7.7). The second ADF was completely absent in the case of the lightly stained h-ADF, pH 7.7, set (Fig. 5 g). The difference in appearance of the second ADF between Fig. 5, d and f, could be due to the difference in binding modes of ADF at different pH. The dark and light staining of the h-ADF–actin filaments in the EM images (Fig. 3, d and f) is due, therefore, to the presence or absence, respectively, of a second ADF molecule bound to many actin subunits.

A second ADF molecule is not apparent in the whole set reconstructions of p-ADF–actin complexes at either pH 6.5 or 7.7 (Fig. 5, c and e). We were able, however, to find traces of the second ADF molecule for the p-ADF complex at pH 7.7. When a subset containing ~15% of these images, isolated using cross-correlation procedures, was reconstructed, a weak density due to the second ADF was observed (data not shown). This suggests that the second site is available for the p-ADF as well, but its occupancy is significantly lower than that of h-ADF.

Binding of ADF Induces a Change in the Tilt of the Actin Subunit

It has been shown that the binding of ADF (Hayden et al., 1993; Hawkins et al., 1993; Ressad et al., 1998) and cofilin (McGough et al., 1997) to F-actin is a cooperative process.

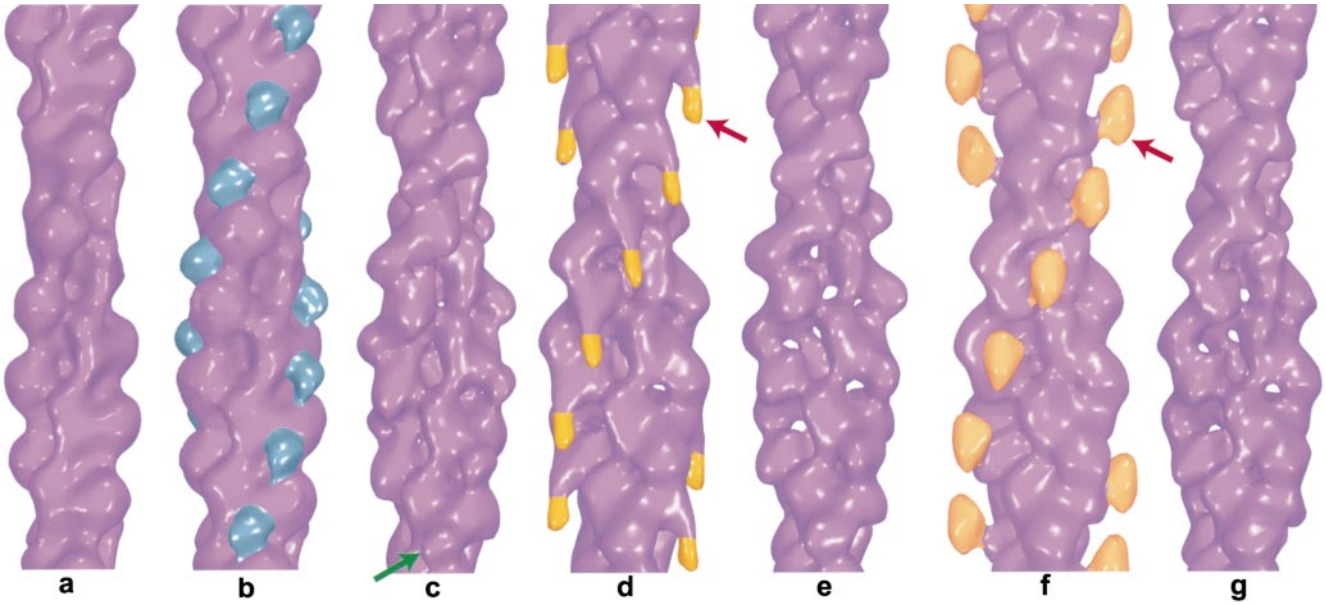

Figure 5. Reconstructed surfaces of h- and p-ADF–actin complexes at pH 6.5 and 7.7. All reconstructions were generated by the IHRSR approach. A reconstruction of pure actin (a) was subtracted from the reconstruction of p-ADF–actin complex at pH 6.5 (c) to generate the density in blue in b due to the primary ADF. This is marked by a green arrow (b and c). The h-ADF–actin complex at pH 6.5 (d), p-ADF–actin complex at pH 7.7 (e), h-ADF–actin darkly stained filaments at pH 7.7 (f), and h-ADF–actin lightly stained filaments at pH 7.7 (g) are shown. A red arrow marks the position of the second ADF molecule bound, and it can be seen that this second molecule is present at low occupancy at pH 6.5 (d) and at higher occupancy at pH 7.7 (f). The difference in appearance of this additional density between d and f (red arrows) is due to a different contact with the F-actin, as well as a difference in occupancy. However, the center of this additional density falls approximately in the same place for both structures.

Because this cooperativity could be transmitted through F-actin itself (Orlova et al., 1995), we were interested to look at regions of the ADF–actin complexes that were either undecorated by ADF or only partially decorated. Using cross-correlation methods (Materials and Methods), we found that ~15% of filament segments used in our reconstructions of ADF–actin (Fig. 5) were more similar to pure actin than ADF–actin. We refer to these segments within ADF-decorated filaments as naked actin. After this initial sorting, traces of the second but not the first ADF molecule could still be seen (data not shown). We used additional sorting procedures, based on iterative cycles of reconstruction and exclusion of images, to isolate segments of ADF–actin filaments that contained mainly undecorated actin to use in the naked actin reconstructions (Fig. 6). Each of these subsets had a mean twist similar to that of the entire ADF–actin complexes, consistent with the notion that the change in twist is propagated in the actin filament beyond the subunits bound by ADF (Blanchoin and Pollard, 1999). However, we were not able to determine the length over which this change in twist persists. Most importantly, the actin subunits within such naked regions are observed to be in a different orientation than they are in pure F-actin. The subunits at pH 6.5 (Fig. 6, a and b) and 7.7 (Fig. 6, c and d) rotate in opposite directions relative to the Holmes model (Holmes et al., 1990) by ~6° and ~12°, respectively. This is observed both for h- (Fig. 6, b and d) and p-ADF (Fig. 6, a and c). As a control, no significant tilt or shift was found when we compared the position of the actin subunits in our reconstructions of pure actin at pH 6.5 and 7.7 with the Holmes model. Atomic models, using rigid body rotations, illustrate this rotation in Fig. 6, e and f. This large change in the tilt of actin subunits at pH 7.7 causes an apparent breakage of the contact between subdomain 4 of one protomer and subdomain 3 of the protomer above it on the same long-pitch strand (Fig. 6 d, red arrow). It also shifts the contact between subdomain 2 of one protomer from subdomain 1 of the subunit above it to subdomain 3 of the subunit above. Overall, the disruption of the longitudinal contacts within the actin filaments may be the most important factor in destabilization of the filament as a result of this tilt of the actin subunit.

Constructing an Atomic Model of F-Actin with Two ADFs Bound per Subunit

We have shown that heterogeneity can exist within the ADF–actin filaments due to variations in twist, the presence of undecorated actin segments, as well as the presence of one or two ADF molecules per actin subunit. We have attempted to eliminate much of this heterogeneity within the set of h-ADF–actin filaments at pH 7.7 and have generated a reconstruction from 2,116 segments found in the center of the twist distribution (162°) that show homogeneity with the respect of having two molecules of h-ADF bound per actin subunit (Fig. 7 a). The second ADF bound was also present in other subsets. Because of the greater homogeneity of this set, both the second ADF and actin are more clearly defined than in the reconstruction of the whole set (Fig. 5 f). Using this volume, it was possible to determine the approximate binding site for the second ADF on actin, and the resulting atomic model is shown in Fig. 7 b. According to our rigid body fitting (assuming no conformational changes in either G-actin or ADF), we predict that residues 22–25, 139–148, and 340–355 of the upper actin subunit and residues 28–29, 44–

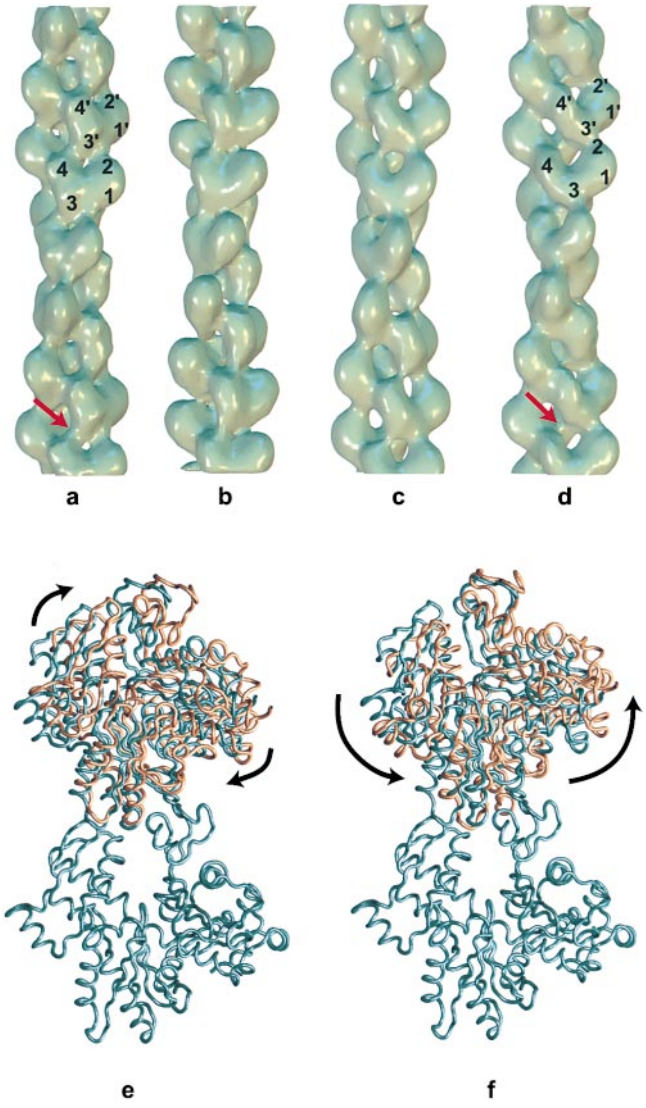

Figure 6. Reconstructions of naked actin from h- and p-ADF–actin complexes at pH 6.5 and 7.7. Within actin filaments decorated with ADF, many segments can be found that appear to contain very little or no ADF. The rendered surfaces generated by IHRSR for such naked actin from p-ADF complex pH 6.5 (a), h-ADF complex, pH 6.5 (b), p-ADF complex, pH 7.7 (c), and h-ADF complex, pH 7.7 (d) are shown. Subdomains 1, 2, 3, and 4 of the actin subunit are labeled, and these domains are labeled as 1′, 2′, 3′, and 4′ on the next subunit along the same long-pitch helical strand. The normal density between subdomain 4 of one subunit and subdomain 3 on an adjacent actin monomer is present at pH 6.5 (a, red arrow), but absent at pH 7.7 (d, red arrow). G-actin subunits were fit (Materials and Methods) to naked F-actin densities from h-ADF set at pH 6.5 (e) and from h-ADF set at pH 7.7 (f). Two adjacent subunits from the symmetry-corrected model of F-actin (Holmes et al., 1990) are shown in cyan as a reference, whereas the fitted structures are shown in brown. Black arrows indicate the tilt of actin subunits away from the position in the Holmes model. The models (e and f) were visualized with the molecular graphics program VMD (Humphrey et al., 1996).

50, and 88–101 of the lower actin subunit (Fig. 7 c) take part in the interaction with the primary ADF molecule. The second ADF molecule does not exhibit strong contacts with actin, although there are near contacts with the actin COOH terminus at helix 359–364 and with helix 112–126 (Fig. 7, b and c). One possibility is that even after sorting images by twist to obtain a homogeneous population, these images had a partial second ADF occupancy that caused a weakening of the density of the second ADF molecule in the reconstruction. It has been suggested that the actin COOH terminus is flexible (Owen and DeRosier, 1993; Orlova and Egelman, 1995), and it is conceivable that small conformational changes of exposed loops and side chains help mediate the contacts between the second bound ADF and F-actin.

Discussion

Variable Twist of F-Actin

It has long been noted that F-actin exhibits a natural variation in crossover spacing (Hanson, 1967). An angular disorder model for this variability was proposed, where the possibility that actin monomers could rotate ~10° from their ideal helical positions was predicted (Egelman et al., 1982). McGough and colleagues (1997) showed that a protein of the ADF/cofilin family changed the mean twist of actin filaments by ~5° per subunit. Initially, it was suggested that changing the twist of actin might cause depolymerization of filaments via a weakening of the longitudinal bonds within the filament, specifically a breaking of the contact between subdomain 2 of the lower subunit with subdomain 1 of the upper subunit in the same long-pitch helix (McGough et al., 1997). It was subsequently shown that, in certain conditions, cofilin disrupted lateral contacts in the actin filament (McGough and Chiu, 1999). Most recently, using a mutant cofilin that changes the twist of actin filaments and fragments them, but does not depolymerize them, it was proposed that the change of twist by itself is not responsible for the enhanced rate of actin subunit dissociation (Pope et al., 2000). So the relationship between the change of twist induced by ADF/cofilin and filament destabilization remains unclear.

In the this work, we used a single particle approach for the analysis of helical structures (Egelman, 2000). The main advantage of this method is the ability to analyze short F-actin segments containing ~12 subunits, without needing to impose a uniform helical symmetry on a long filament. This has allowed us to address many issues of heterogeneity in both the twist of F-actin and the binding by ADF that have not been possible using conventional methods. We found that segments of F-actin by itself, without ADF/cofilin proteins, could exist in the state of 162° twist observed for cofilin-decorated F-actin. Remarkably, we were able to find ~8% of the segments that had a mean twist of 158°, a change by ~8° per subunit from the mean twist of the whole set. We have suggested that the variability in twist within actin filaments is not continuous, but rather that subunits might exist in only a few discrete states (Orlova and Egelman, 2000). This model predicts a relatively static disorder, rather than the thermal torsional motions predicted by a continuous variability of twist. Although at this point we do not have any information about the number of such discrete states, or their distribution, our observation of many segments having a mean twist of ~158° suggests several points. It is likely that one state of twist is ~158°. Another conclusion is that there must be a

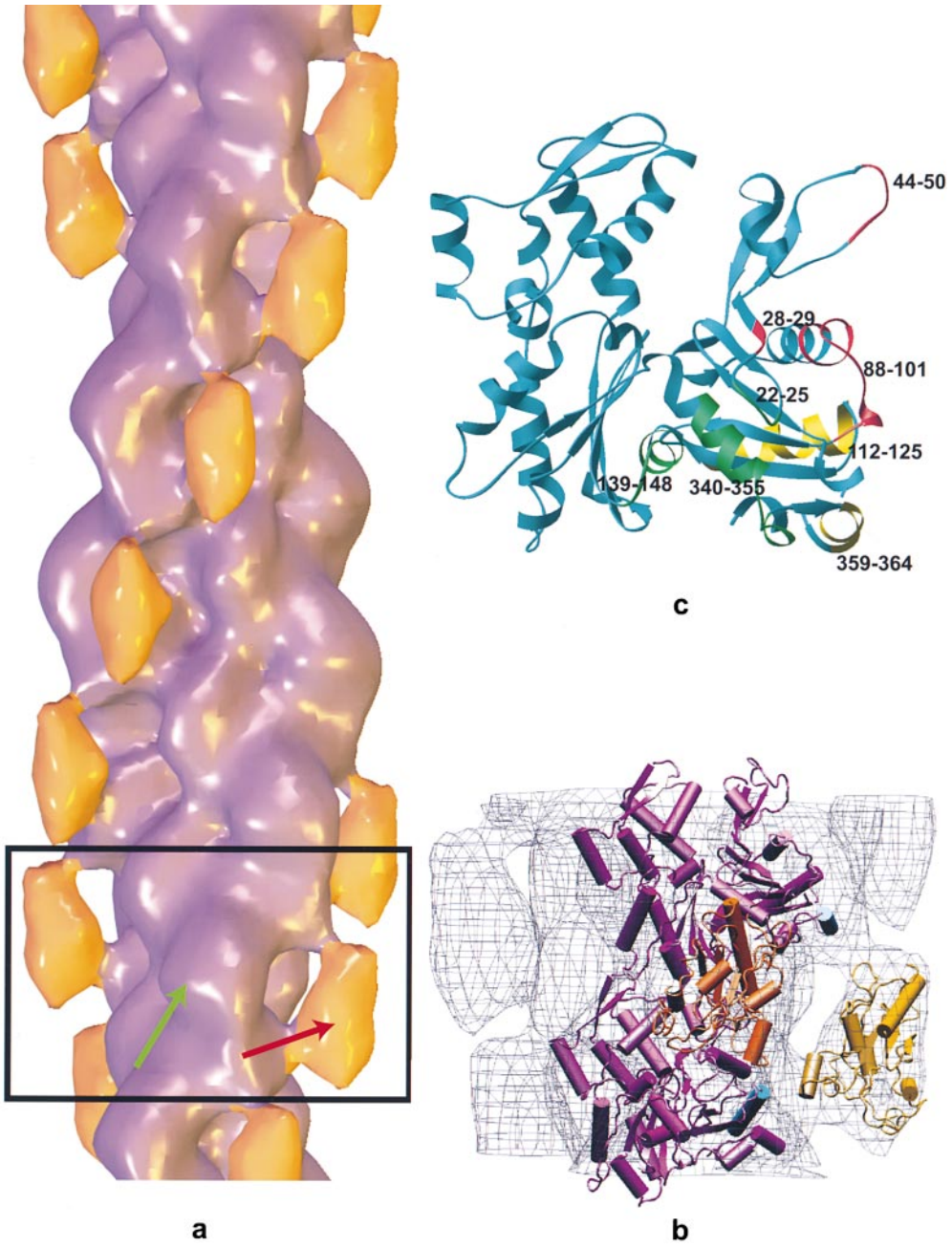

Figure 7. Atomic model of doubly ADF-decorated F-actin. (a) Rendered surface of the h-ADF–actin complex at pH 7.7, generated from a homogeneous subset of 2,116 segments. Green and red arrows mark position of the first and the second ADF molecules, respectively. (b) Atomic model of F-actin decorated with two h-ADF molecules per subunit. The isocontour of the EM density map is shown as a gray wire mesh. Two adjacent actin subunits are shown in purple. The weakly and strongly attached ADF structures (Hatanaka et al., 1996) are shown in yellow and orange, respectively. Proposed weak contacts with two helices of actin are shown in cyan: actin's COOH terminal helices 359–364 (upper monomer), and helices 112–126 (lower monomer). Atomic coordinates of the model are available from the corresponding author. (c) Ribbon diagram of actin molecule, with putative ADF contacts indicated as follows: red, lower monomer contacts; green, upper monomer contacts; and yellow, contacts with the second ADF molecule. Numbers of residues that are involved in the interaction with ADF are indicated.

cooperativity in twist within the filament, so that the probability of a subunit having a particular twist is dependent on the twist of adjacent subunits. If twist states were randomly distributed, we would expect to see a nearly Gaussian distribution for the mean twist of 12 subunits (from the central limit theorem), and we clearly do not (Fig. 1 b). Attempting to describe the actin filament in terms of a Markov model of twist probabilities dependent on the twist of adjacent subunits must still wait for more detailed information.

When the IHRSR method is applied to ADF–actin complexes, we observe a large reduction in the variability of twist of these filaments when compared with pure F-actin filaments. Consistent with what we observe for pure F-actin, we suggest that ADF/cofilin proteins stabilize an already existing state of twist of the actin filament rather than imposing a new one.

Two Molecules of ADF per Actin Subunit

Also, we have been able to see that one component of variability in the binding of ADF to actin is due to whether one ADF molecule or two bind per actin subunit. The distribution of these two possibilities is different between the h- and p-ADF. Under similar conditions at pH 7.7, the h-ADF–actin complex segments are more likely to be found in the 2:1 stoichiometry of binding than the p-ADF–actin complex.

ADF/cofilin proteins from different sources have different depolymerizing activities and for the majority of these proteins this activity is pH dependent (Yonezawa et al., 1985). The rate of actin depolymerization also depends on the isoform of actin. It was reported that UNC-60B from *Caenorhabditis elegans* disrupted *C. elegans* F-actin more efficiently than it disrupted rabbit muscle actin (Ono et al.,

1999). On the other hand, *Acanthamoeba* actophorin depolymerizes rabbit F-actin faster than it depolymerizes *Acanthamoeba* actin (Maciver et al., 1998). h-ADF is more efficient in disrupting rabbit muscle actin filaments than is p-ADF (Ressad et al., 1998). To look at the structural basis for these differences, as well as to understand the mechanism of filament destabilization, we investigated h- and p-ADF–actin complexes with F-actin at high and low pH. One of the most important observations was the presence of a second ADF molecule bound to actin filaments. This can be easily observed with h-ADF at pH 7.7, when ADF is active in filament destabilization, but is also present more weakly with p-ADF at the same pH. We suggest that the greater efficiency observed for h-ADF compared with p-ADF in depolymerizing actin (Ressad et al., 1998) is due to the higher affinity of h-ADF for occupying the second binding site on actin. We were able to sort filament images containing the second ADF bound at the level of the raw micrographs, due to the different staining of these filaments (Fig. 3, d and f). The absence of filaments containing long regions with both light and dark staining suggests a large cooperativity in the binding of the second ADF molecule that extends over an entire filament. This is similar to what has previously been observed in the binding of heavy meromyosin to actin (Orlova and Egelman, 1997).

Although the binding of two ADF molecules per actin subunit has not been previously described, it is not inconsistent with previous observations. A stoichiometry of 1.3:1 for the interaction of h-ADF with rabbit F-actin at pH 6.5 was observed (Hawkins et al., 1993). This is consistent with our reconstruction for this complex in which only traces of the second ADF can be seen (Fig. 5 d). It was postulated (Hawkins et al., 1993) that there is no interaction between h-ADF and F-actin at pH higher than 7.5, where we can observe the 2:1 stoichiometry of binding more fully. But this is also consistent with our EM observations, since after 10 min of incubation there is no F-actin left because of the high depolymerizing activity of ADF at this pH. Even during a short incubation time (4 min on the grid) at pH 7.7, ADF was able to depolymerize approximately half of the F-actin (with a total actin concentration of 2 μM), and only short fully occupied filaments were observed by EM.

The second binding site for ADF is also in agreement with biochemical observations, even though many of the molecular details of the ADF–cofilin interaction with actin are still unknown. Using biochemical and genetic approaches, several sites on actin were predicted to be important for the interaction between these proteins. Chemical cross-linking was used to propose that residues 1–12 on actin's NH_2 terminus and residues 357–375 on the COOH terminus were involved in the interaction with the homologous starfish protein depactin (Sutoh and Mabuchi, 1986, 1989). It was shown that residues 334–336, 290–292, 326, and 328 of actin could be involved in the interaction with cofilin in yeast (Rodal et al., 1999). It was also suggested that residues 75–105 and 112–125 of rabbit muscle actin might interact with human cofilin (Renoult et al., 1999). The previously determined low resolution structure of the actin–cofilin filament displayed only general agreement with these data and predicted that residues 143–149, 345–346, 349–351, and 354 of the actin upper monomer and residues 21, 28, 36–38, 40–43, 49–54, 57, 61, 87–88, 90–96, and 101 of the lower monomer were involved in the interaction with cofilin. Since the helix containing residues 112–125 in actin is on the opposite side of the actin subunit from the position of the bound cofilin observed by McGough et al. (1997), a model of "intercalated" binding was proposed by Renoult et al. (1999). The COOH terminus of actin, suggested to be involved in the binding of ADF/cofilin proteins (Sutoh and Mabuchi, 1986), is also on the opposite side of the actin subunit. Our visualization of a second ADF bound to actin in the region of both helix 112–125 and the COOH terminus reconciles these observations, without needing to greatly change the mode of binding of the first ADF molecule from that described by McGough et al. (1997).

We suggest several reasons why a second cofilin molecule was not seen in previous EM studies of actin–cofilin complexes (McGough et al., 1997; McGough and Chiu, 1999; Pope et al., 2000). First, platelet F-actin was used in those studies, whereas we used rabbit muscle actin. As mentioned above, the isoform of actin can strongly influence the biochemical characteristics of the ADF–actin interaction. Platelet F-actin is more resistant to the depolymerization activity of human cofilin than rabbit F-actin. When rabbit F-actin was used after 30–90-min incubation on ice, they observed only short actin filaments that were useless in helical approaches (McGough et al., 1997). Second, the model for the cofilin–F-actin complex proposed by McGough et al. (1997) was based on experiments performed at pH 6.5, when this complex is stable. We observed the second molecule predominantly at pH 7.7, where actin is more easily deploymerized. Third, human cofilin shares only 70% homology with h-ADF (Bamburg, 1999) and could have a lower affinity for the second binding site.

Variable Tilt of Actin Subunits

Under conditions where F-actin is readily destabilized by h-ADF (pH 7.7), we can observe segments of naked actin where the subunits have undergone a large (~12°) tilt from their position in normal F-actin. This tilt appears to break the longitudinal bounds in the long-pitch helices. Since this tilt is much more striking in these naked segments than in the fully decorated F-actin, either this conformation occurs after ADF binds and dissociates from these regions or is induced by the binding of ADF to neighboring subunits. The possibility of a variable tilt of the actin subunit within the filament has been raised previously (Egelman and DeRosier, 1983; Tilney et al., 1983). In stereocilia of the inner ear, it was suggested that the ability of actin subunits to tilt by ~10° could explain the tilting of cross-bridges between actin filaments observed when these bundles bend (Tilney et al., 1983). Although actin filaments in muscle only undergo an extension of ~0.08 Å per subunit on average when full tension is induced (Huxley et al., 1994; Wakabayashi et al., 1994), relatively large axial perturbations of mass within F-actin can be seen by both x-ray diffraction (Lednev and Popp, 1990) and EM (Egelman and DeRosier, 1983) when filaments are packed into bundles. It was estimated that these displacements in axially projected mass could be roughly ±3 Å (Egelman and DeRosier, 1983), and the suggestion was made that a variable tilt of the subunits could recon-

cile such displacements with the relatively fixed average axial spacing. A comparison between our model for a subunit with a 12° tilt and the Holmes model (Holmes et al., 1990) shows that the axially projected mass distribution would shift by ~4 Å between the two. It is striking that the magnitude of the tilt previously predicted, in both angular range and projected axial shift, is quite similar to what we now observe.

It was proposed that the untwisting of actin by cofilin could disrupt the contacts between subdomain 2 of the lower subunit and subdomain 1 of the upper one, thus destabilizing the actin filament (McGough et al., 1997). The large tilt of the actin subunits is induced by ADF under conditions where filaments are readily depolymerized, and this tilt appears to make even greater changes in actin subunit–subunit contacts within the filament. Specifically, a large contact between subdomain 4 of one subunit and subdomain 3 of the subunit above is broken. We think it likely that this disruption of the normal structure of F-actin could be responsible for the destabilization of the filament and lead to either filament breakage, if it occurs, within filaments or subunit dissociation, if it occurs, at the ends of filaments.

Conclusions

The variable twist of F-actin allows segments of filaments to randomly exist in the same state of twist induced by ADF/cofilin in the absence of these proteins. The binding of ADF to actin causes cooperative changes in both F-actin tilt and twist to be propagated to actin subunits that are undecorated. The binding of two molecules of ADF per actin subunit reconciles previous biochemical observations with structural models. The depolymerization activity of ADF/cofilin may be due to both changes in the tilt and twist of actin subunits, and this may occur mainly after two molecules of ADF are bound per actin.

This work was supported by National Institutes of Health grants R01-AR42023 (E.H. Egelman) and P41-RR12255 (W. Wriggers).

Submitted: 8 December 2000
Revised: 1 February 2001
Accepted: 5 February 2001

References

Bamburg, J.R. 1999. Proteins of the ADF/cofilin family: essential regulators of actin dynamics. *Annu. Rev. Cell Dev. Biol.* 15:185–230.

Bamburg, J.R., A. McGough, and S. Ono. 1999. Putting a new twist on actin: ADF/cofilins modulate actin dynamics. *Trends Cell Biol.* 9:364–370.

Bernstein, B.W., W.B. Painter, H. Chen, L.S. Minamide, H. Abe, and J.R. Bamburg. 2000. Intracellular pH modulation of ADF/cofilin proteins. *Cell Motil. Cytoskeleton.* 47:319–336.

Blanchoin, L., and T.D. Pollard. 1999. Mechanism of interaction of *Acanthamoeba* actophorin (ADF/Cofilin) with actin filaments. *J. Biol. Chem.* 274: 15538–15546.

Carlier, M.F. 1998. Control of actin dynamics. *Curr. Opin. Cell Biol.* 10:45–51.

Carlier, M.F., and D. Pantaloni. 1997. Control of actin dynamics in cell motility. *J. Mol. Biol.* 269:459–467.

Carlier, M.F., V. Laurent, J. Santolini, R. Melki, D. Didry, G.X. Xia, Y. Hong, N.H. Chua, and D. Pantaloni. 1997. Actin depolymerizing factor (ADF/cofilin) enhances the rate of filament turnover: implication in actin-based motility. *J. Cell Biol.* 136:1307–1322.

Chen, H., B.W. Bernstein, and J.R. Bamburg. 2000. Regulating actin-filament dynamics in vivo. *Trends Biochem. Sci.* 25:19–23.

Cooper, J.A., J.D. Blum, R.C. Williams, Jr., and T.D. Pollard. 1986. Purification and characterization of actophorin, a new 15,000-dalton actin-binding protein from *Acanthamoeba castellanii*. *J. Biol. Chem.* 261:477–485.

Drummond, D.R., M. Peckham, J.C. Sparrow, and D.C. White. 1990. Alteration in crossbridge kinetics caused by mutations in actin. *Nature.* 348:440–442.

Du, J., and C. Frieden. 1998. Kinetic studies on the effect of yeast cofilin on yeast actin polymerization. *Biochemistry.* 37:13276–13284.

Egelman, E.H. 2000. A robust algorithm for the reconstruction of helical filaments using single-particle methods. *Ultramicroscopy.* 85:225–234.

Egelman, E.H., and D.J. DeRosier. 1983. Structural studies of F-actin. *In* Actin: Structure and Function in Muscle and Non-Muscle Cells. C. dos Remedios, editor. Academic Press Inc., Orlando, FL. 17–24.

Egelman, E.H., N. Francis, and D.J. DeRosier. 1982. F-actin is a helix with a random variable twist. *Nature.* 298:131–135.

Hanson, J. 1967. Axial period of actin filaments: electron microscope studies. *Nature.* 213:353–356.

Hatanaka, H., K. Ogura, K. Moriyama, S. Ichikawa, I. Yahara, and F. Inagaki. 1996. Tertiary structure of destrin and structural similarity between two actin-regulating protein families. *Cell.* 85:1047–1055.

Hawkins, M., B. Pope, S.K. Maciver, and A.G. Weeds. 1993. Human actin depolymerizing factor mediates a pH-sensitive destruction of actin filaments. *Biochemistry.* 32:9985–9993.

Hayden, S.M., P.S. Miller, A. Brauweiler, and J.R. Bamburg. 1993. Analysis of the interactions of actin depolymerizing factor with G- and F-actin. *Biochemistry.* 32:9994–10004.

Holmes, K.C., D. Popp, W. Gebhard, and W. Kabsch. 1990. Atomic model of the actin filament. *Nature.* 347:44–49.

Humphrey, W., A. Dalke, and K. Schulten. 1996. VMD: visual molecular dynamics. *J. Mol. Graph.* 14:33–38.

Huxley, H.E., A. Stewart, H. Sosa, and T. Irving. 1994. X-ray diffraction measurements of the extensibility of actin and myosin filaments in contracting muscle. *Biophys. J.* 67:2411–2421.

Kim, E., E. Bobkova, C.J. Miller, A. Orlova, G. Hegyi, E.H. Egelman, A. Muhlrad, and E. Reisler. 1998. Intrastrand cross-linked actin between Gln-41 and Cys-374. III. Inhibition of motion and force generation with myosin. *Biochemistry.* 37:17801–17809.

Lappalainen, P., E.V. Fedorov, A.A. Fedorov, S.C. Almo, and D.G. Drubin. 1997. Essential functions and actin-binding surfaces of yeast cofilin revealed by systematic mutagenesis. *EMBO (Eur. Mol. Biol. Organ.) J.* 16:5520–5530.

Lednev, V.V., and D. Popp. 1990. Supercoiling of F-actin filaments. *J. Struct. Biol.* 103:225–231.

Maciver, S.K., H.G. Zot, and T.D. Pollard. 1991. Characterization of actin filament severing by actophorin from *Acanthamoeba castellanii*. *J. Cell Biol.* 115:1611–1620.

Maciver, S.K., B.J. Pope, S. Whytock, and A.G. Weeds. 1998. The effect of two actin depolymerizing factors (ADF/cofilins) on actin filament turnover: pH sensitivity of F-actin binding by human ADF, but not of *Acanthamoeba* actophorin. *Eur. J. Biochem.* 256:388–397.

McGough, A., and W. Chiu. 1999. ADF/cofilin weakens lateral contacts in the actin filament. *J. Mol. Biol.* 291:513–519.

McGough, A., B. Pope, W. Chiu, and A. Weeds. 1997. Cofilin changes the twist of F-actin: implications for actin filament dynamics and cellular function. *J. Cell Biol.* 138:771–781.

Moriyama, K., and I. Yahara. 1999. Two activities of cofilin, severing and accelerating directional depolymerization of actin filaments, are affected differentially by mutations around the actin-binding helix. *EMBO (Eur. Mol. Biol. Organ.) J.* 18:6752–6761.

Ono, S., D.L. Baillie, and G.M. Benian. 1999. UNC-60B, an ADF/cofilin family protein, is required for proper assembly of actin into myofibrils in *Caenorhabditis elegans* body wall muscle. *J. Cell Biol.* 145:491–502.

Orlova, A., and E.H. Egelman. 1995. Structural dynamics of F-actin. I. Changes in the C-terminus. *J. Mol. Biol.* 245:582–597.

Orlova, A., and E.H. Egelman. 1997. Cooperative rigor binding of myosin to actin is a function of F-Actin structure. *J. Mol. Biol.* 265:469–474.

Orlova, A., and E.H. Egelman. 2000. F-actin retains a memory of angular order. *Biophys. J.* 78:2180–2185.

Orlova, A., E. Prochniewicz, and E.H. Egelman. 1995. Structural dynamics of F-actin. II. Co-operativity in structural transitions. *J. Mol. Biol.* 245:598–607.

Owen, C., and D. DeRosier. 1993. A 13 A map of the actin–scruin filament from the limulus acrosomal process. *J. Cell Biol.* 123:337–344.

Pollard, T.D., L. Blanchoin, and R.D. Mullins. 2000. Molecular mechanisms controlling actin filament dynamics in nonmuscle cells. *Annu. Rev. Biophys. Biomol. Struct.* 29:545–576.

Pope, B.J., S.M. Gonsior, S. Yeoh, A. McGough, and A.G. Weeds. 2000. Uncoupling actin filament fragmentation by cofilin from increased subunit turnover. *J. Mol. Biol.* 298:649–661.

Prochniewicz, E., and T. Yanagida. 1990. Inhibition of sliding movement of F-actin by cross-linking emphasizes the role of actin structure in the mechanism of motility. *J. Mol. Biol.* 216:761–772.

Renoult, C., D. Ternent, S.K. Maciver, A. Fattoum, C. Astier, Y. Benyamin, and C. Roustan. 1999. The identification of a second cofilin binding site on actin suggests a novel, intercalated arrangement of F-actin binding. *J. Biol. Chem.* 274:28893–28899.

Ressad, F., D. Didry, G.X. Xia, Y. Hong, N.H. Chua, D. Pantaloni, and M.F. Carlier. 1998. Kinetic analysis of the interaction of actin-depolymerizing factor (ADF)/cofilin with G- and F-actins. Comparison of plant and human ADFs and effect of phosphorylation. *J. Biol. Chem.* 273:20894–20902.

Rodal, A.A., J.W. Tetreault, P. Lappalainen, D.G. Drubin, and D.C. Amberg.

1999. Aip1p interacts with cofilin to disassemble actin filaments. *J. Cell Biol.* 145:1251–1264.

Saxton, W.O., and W. Baumeister. 1982. The correlation averaging of a regularly arranged bacterial cell envelope protein. *J. Microsc.* 127:127–138.

Schwyter, D.H., S.J. Kron, Y.Y. Toyoshima, J.A. Spudich, and E. Reisler. 1990. Subtilisin cleavage of actin inhibits in vitro siding movement of actin filaments over myosin. *J. Cell Biol.* 111:465–470.

Strzelecka-Golaszewska, H., E. Prochniewicz, E. Nowak, S. Zmorzynski, and W. Drabikowski. 1980. Chicken-gizzard actin: polymerization and stability. *Eur. J. Biochem.* 104:41–52.

Sutoh, K., and I. Mabuchi. 1986. Improved method for mapping the binding site of an actin-binding protein in the actin sequence. Use of a site-directed antibody against the N-terminal region of actin as a probe of its N-terminus. *Biochemistry.* 25:6186–6192.

Sutoh, K., and I. Mabuchi. 1989. End-label finger printings show that an N-terminal segment of depactin participates in interaction with actin. *Biochemistry.* 28:102–106.

Theriot, J.A. 1997. Accelerating on a treadmill: ADF/cofilin promotes rapid actin filament turnover in the dynamic cytoskeleton. *J. Cell Biol.* 136:1165–1168.

Tilney, L.G., E.H. Egelman, D.J. DeRosier, and J.C. Saunder. 1983. Actin filaments, stereocilia, and hair cells of the bird cochlea. II. Packing of actin filaments in the stereocilia and in the cuticular plate and what happens to the organization when the stereocilia are bent. *J. Cell Biol.* 96:822–834.

van Gunsteren, W.F., and H.J.C. Berendsen. 1977. Algorithms for macromolecular dynamics and constraint dynamics. *Mol. Physics.* 34:1311–1327.

Van Troys, M., D. Dewitte, J.L. Verschelde, M. Goethals, J. Vandekerckhove, and C. Ampe. 1997. Analogous F-actin binding by cofilin and gelsolin segment 2 substantiates their structural relationship. *J. Biol. Chem.* 272:32750–32758.

Wakabayashi, K., Y. Sugimoto, H. Tanaka, Y. Ueno, Y. Takezawa, and Y. Amemiya. 1994. X-ray diffraction evidence for the extensibility of actin and myosin filaments during muscle contraction. *Biophys. J.* 67:2422–2435.

Wriggers, W., S. Birmanns. 2001. Using Situs for flexible and rigid-body fitting of multi-resolution single molecule data. *J. Struct. Biol.* In Press.

Wriggers, W., and K. Schulten. 1999. Investigating a back door mechanism of actin phosphate release by steered molecular dynamics. *Proteins.* 35:262–273.

Wriggers, W., R.A. Milligan, K. Schulten, and J.A. McCammon. 1998. Self-organizing neural networks bridge the biomolecular resolution gap. *J. Mol. Biol.* 284:1247–1254.

Wriggers, W., R.A. Milligan, and J.A. McCammon. 1999. Situs: a package for docking crystal structures into low-resolution maps from electron microscopy. *J. Struct. Biol.* 125:185–195.

Yonezawa, N., E. Nishida, and H. Sakai. 1985. pH control of actin polymerization by cofilin. *J. Biol. Chem.* 260:14410–14412.

Yonezawa, N., E. Nishida, K. Iida, H. Kumagai, I. Yahara, and H. Sakai. 1991. Inhibition of actin polymerization by a synthetic dodecapeptide patterned on the sequence around the actin-binding site of cofilin. *J. Biol. Chem.* 266: 10485–10489.